Resources, Conservation and Recycling 132 (2018) 204–217

Contents lists available at ScienceDirect

Resources, Conservation and Recycling

journal homepage: www.elsevier.com/locate/resconrec

Full length article

An urban climate assessment and management tool for combined heat and air quality judgements at neighbourhood scales

Gert-Jan Steeneveld[a,*], Jochem O. Klompmaker[b], Ronald J.A. Groen[b], Albert A.M. Holtslag[a]

[a] Wageningen University, Meteorology and Air Quality Section, PO Box 47, 6700 AA Wageningen, The Netherlands
[b] Witteveen+Bos consulting engineers, PO Box 233, 7400 AE Deventer, The Netherlands

ARTICLE INFO

Article history:
Received 16 February 2016
Received in revised form 18 June 2016
Accepted 7 December 2016
Available online 29 December 2016

Keywords:
Urban heat island
Air quality
Mortality
Weather research and forecasting model
Urban climate index
Health

ABSTRACT

Meteorology and air quality are key aspects for city life and urban metabolism. Both aspects build upon urban and natural processes, involve stocks and flows of heat and pollution, with in the end consequences for stocks and flows concerning other urban entities and processes such as human outdoor activities, leisure, transport modes, as well as for urban design and planning. During hot summer days cities experience an urban heat island effect mainly at the start of the evening and at night. As a result inhabitants might be subject to a reduced human thermal comfort. Hot summer days often also coincide with relatively poor air quality conditions. Both short-term effects are known to increase the mortality rates, and it is challenging to distinguish their impacts on health effects. Moreover, climate change scenarios indicate an enhancement of future heat wave frequency and intensity and a further deterioration of human thermal comfort. These issues raise the need and the urgency for city adaptation, but an integrated method for the assessment is still missing. Effective city adaptation is hampered by the complexity of the urban climate (induced by both meteorology and urban morphological characteristics) and its potential health risks, combined with the complex spatial interaction of stakeholders and economical functions. To warn the general public, and to effectively perform urban planning interventions, straightforward environmental indicators are required. Indicators have been developed for the individual aspects before, but indices that combine both air quality and urban heat are rather scarce (Rainham and Smoyer-Tomic, 2003). This study develops a novel metric that combines the impact of thermal comfort and air quality by accounting for the relative health risk for both aspects. A straightforward quantification method for this metric has been developed to provide an objective, rational assessment. The application of this new Urban Climate assessment tool is then applied to a case study for a heat wave in the Northwestern Europe, and applied for a sample intervention in the city center of Ghent (Belgium).

1. Introduction

Urban areas are sophisticated entities characterised by both a complex physical environment containing a variety of urban morphology and urban fabric, as well as a social environment where citizens live, work, travel and recreate. In order to understand urban developments at different spatial and temporal scales, both natural and man-made contributions to the urban systems and their interactions should be analysed. The urban metabolism model facilitates the description and analysis of the flows of the materials and energy within cities. It is a figurative framework to study the interactions of natural and human systems. For example Dijst (2013) presents a flow perspective on urban and natural systems, covering stocks and flows of both natural and anthropogenic origin. In such perspective, urban processes of varying temporal scales, such as land use design, population, housing, employment and travel, can be linked to natural processes. As an example on how these natural processes interact with urban traffic flows, Böcker and Thorsson (2014) studied the role of weather effects on cycling frequencies, cycling durations, and the exchange between cycling and other transport modes. They report negative effects of precipitation and wind speed, and a nonlinear bell-shaped relation between thermodynamic variables on cycling and opposite effects on car usage. In addition, Helbich et al. (2014) shows that these relation are stronger for leisure trips than for work travels. Moreover they report that the

* Corresponding author.
E-mail address: Gert-Jan.Steeneveld@wur.nl (G.-J. Steeneveld).

https://doi.org/10.1016/j.resconrec.2016.12.002

significance of weather effects varies, specifically across settlement density.

The current study analyses overall (i.e. combination of both indoor and outdoor) exposures to naturally varying weather conditions and the added influences by anthropogenic contributions via the built environment, release of air pollution and in the long term via climate change. The exposure will be related to urban morphology and as such the study integrates natural and social sciences. We particularly concentrate on the budgets and flows of urban heat and air pollution.

Urban areas experience a different meteorology than the rural surroundings. Especially for clear sky and calm conditions cities are up to several degrees warmer than the countryside (Oke, 1982). These urban heat islands (UHI) are present in almost all urban areas and even relatively small towns may experience such an effect (Steeneveld et al., 2011a). The main causes of the UHI relate to structural and land cover differences between urban and rural areas (Stewart and Oke, 2012). Cities as a whole typically have a smaller albedo than rural areas. In addition, the sky view of the surface in urban areas is limited by buildings. Therefore there is a restricted emission of thermal radiation to space at night. Also, fabric, concrete and asphalt have a higher heat capacity than rural areas, resulting in a reduced cooling after sunset during the night. Moreover anthropogenic activities such as human metabolism, traffic, heating and cooling demand by buildings, electricity, and industry result in heat emissions (Souch and Grimmond, 2006; Krpo et al., 2010).

In addition to the heat effects, these weather conditions also support high atmospheric pollutant concentrations, in particular nitrogen oxides, ozone. The diurnal cycle of air quality is caused by both the dynamics of the atmospheric boundary layer and atmospheric chemistry. The boundary layer is shallow (50–200 m) during the early morning before sunrise. After sunrise the land surface is heated by solar radiation that consequently trigger atmospheric turbulence to grow the boundary layer to typical values of 1000–2000 m at the end of the afternoon. Hence pollutants are being diluted over a deeper layer at the end of the afternoon, and thereby diluting the concentrations. On the other hand the atmospheric chemistry of the ozone cycle is perturbed by release of ozone precursors by traffic, i.e. NOx, CO and volatile organic compounds in the rush hour. Once the sun reaches its maximum elevation the chemical processes are started due to the high radiation intensity which net converts the NOx to potentially harmful ozone concentrations in a time scale of 30 min to 1 h. The diurnal cycle of particulate matter peaks typically during the morning and afternoon rush hours, since motorized traffic is the main source in cities. This is on top of the fact that clear sky and calm conditions involve subsidence that traps the pollutants in the atmospheric boundary layer below the inversion. The occurrence of these processes on a regional/continental scale accumulate into a stock of air pollution which is (slowly) transported, which for the Northwestern Europe results in high peaks of advected air pollution. Both the raised pollutant concentrations and the urban heat island effect result in adverse health effects (Rainham and Smoyer-Tomic 2003;Tan et al., 2010) and reduced labour productivity (Hanna et al., 2011; Zander et al., 2015).

An enhanced understanding of the combined effects of the diurnal cycle of urban heat and air quality may affect citizens activities in order to minimize health effects. This would imply that outdoor activities should be planned in the early morning, and indoor activities are preferred during the day. The daily mobility patterns for cyclists and pedestrians should be adjusted as well, i.e. going to work earlier than normal during episodes. On the other hand mobility patterns from cars could be managed in such away that the precursors of ozone are emitted as least as possible.

The association between high temperatures and natural mortality has been documented several times (Smoyer, 1998; Baccini et al., 2008; Analitis et al., 2008; Anderson and Bell, 2009). The relation has often been shown as so called V- or J-shaped function, with the lowest mortality rates at moderate temperatures and rising progressively as temperatures increase or decrease (Huynen et al., 2001; Curriero et al., 2002). In the light of climate change this relation is a matter of increasing concern (e.g. Molenaar et al., 2016). The heat wave in 2003 in Western Europe has received much attention in particular. Several countries registered considerably elevated mortality numbers (Vandentorren et al., 2004, 2006; Conti et al., 2005; Garssen et al., 2005; Smargiassi et al., 2009).

In densely populated regions, the social, political, and economic space that separates cities and countryside are no longer distinguished by a clear urban–rural division (Stewart and Oke, 2012). Therefore it is hard to describe unique 'urban' and unique 'rural' reference states, and thus to unambiguously determine the UHI effect. Neighbourhoods can vary widely in their characteristics that influence the UHI. At the same time, rural conditions may vary across climate zones. In the remainder of the paper, UHI will refer to the temperature difference between urban local climate zones and the rural climate zone D (low grass, Stewart and Oke, 2012). Adaptation measures to minimize the UHI can range from modification of city design strategy and building material or introduction of vegetation (Synnefa et al., 2008; Mills, 2009), though its efficiency may vary with the present urban morphological structure. A quantification and assessment of the elevated health risk, caused by the UHI, can provide insight in the efficiency of adaptive measures (Bohnenstengel and co-authors, 2015). At the same time, one should realize that heatwave episodes often coincide with relative poor air quality. Hence the individual contributions of high temperatures and poor air quality to the mortality have not been unravelled. Also, a metric that combines these contributions is currently lacking.

In this paper we use a meteorological modelling study to investigate the effect of urban morphological parameters on UHI for a heat wave episode in 2006 in northwestern Europe. To assess health risks by high temperature, an analogue with the health risk of short-term exposure to ozone is made, and a single index for the combined effect is developed. In addition, the contribution of health risk by high temperatures is subdivided by a rural and an urban contribution. As such, a better scientific understanding of the health effects of combined exposure may assist in urban planning. This paper is organized as follows; Section 2 presents background material on the topic at hand and Section 3 outlines the methodology. Section 4 presents the results, and Sections 5 and 6 provide a discussion and concluding remarks.

2. Background

2.1. Heat index

The temperature in the city during a heat wave is determined by weather conditions at the regional level and the local urban environment. To assess health effects of heat in the city therefore two aspects are important, namely how public health risk increase as it gets warmer, and how the urban environment increases the risk or worsen the effects. We note that temperature alone is not sufficient to estimate heat stress, i.e. one has to consider all processes that affect the human energy balance and that may result in an unpleasant body temperature, like radiation, humidity, and wind speed play a role (Budd, 2001). To estimate heat stress, a variety of thermal indices have been developed. Examples are the wet bulb globe temperature that linearly combines air temperature and vapour pressure and the mean radiant temperature that

expresses all incoming radiation on the human body in a single temperature. A more advanced metric is the physiological equivalent temperature that is based on a model for the human energy balance (Höppe, 1999). Recently the Universal Thermal Climate Index (UTCI, Jendritzky et al., 2012) has been developed from first principles of the human energy balance (see www.utci.org). Lower thresholds of this index indicating heat stress are 26 °C (moderate heat stress), 32 °C (strong heat stress) and 38 °C (very strong heat stress). For night-time conditions a limit value of the UTCI can be set at 15 °C and exceeding of this value (between 10:00 p.m. to 4:00 p.m.) is expected also to lead to heat stress.

In this study we will relate adverse human comfort to mortality in a practical way, using straightforward and routinely available meteorological data. Relations between mortality and UTCI have not been established yet, and moreover UTCI estimation from routine weather data is not straightforward. Therefore an alternative approach will be followed in Section 3.

2.2. Air quality index

An Air Quality Index (AQI) indicates the pollution level of the ambient environment, and what associated health effects might be a concern. Typically an AQI focuses on health effects one may experience within a few hours or days after breathing polluted air. The US Environmental Protection Agency (EPA) calculates the AQI on basis of five major air pollutants regulated by the Clean Air Act: ground-level ozone, particle pollution (also known as particulate matter), carbon monoxide, sulphur dioxide, and nitrogen dioxide. For each of these pollutants, EPA has established national air quality standards to protect public health (EPA, 2015). In the Netherlands and many other countries, ground-level ozone and airborne particles are the two pollutants that often pose the greatest threat to human health and these are used here as main indicators.

In order to protect public health, EPA has set an AQI value of 100 as the national air quality standard for pollutants. AQI values below 100 are generally thought of as satisfactory. When AQI values are above 100, air quality is considered to be unhealthy-at first for certain sensitive groups of people and subsequently for everyone as AQI values get higher. For example, an AQI = 50 represents good air quality with little potential to affect public health, while an AQI > 300 represents hazardous air quality. To facilitate a user-friendly interpretation, the AQI has been divided into six categories. To present the air quality situation in European cities in a comparable and comprehensive way, all detailed measurements are transformed into a single relative metric: the Common Air Quality Index (CAQI). Three different indices have been developed by CiteAir to enable the comparison of three different time scales: a) An hourly index, which describes the air quality today, b) a daily index, which stands for the general air quality situation of yesterday as based on daily values and updated once a day, and c) finally an annual index which represents the city's general air quality conditions throughout the year and how it compares to European air quality norms. This study will use daily mean and 8 h mean concentrations in the formulation of an air quality index, and finally a more general urban climate index that is formulated such that 100 represents a reference state.

3. Methodology

This section first describes the selected urban morphological properties that have been explored. Then the setup of the meteorological model simulation is summarized. Subsequently the methodology to quantify health risks due to urban heat and air quality are presented.

3.1. Local climate zones

This study aims to develop a combined index for human thermal comfort and air quality. These atmospheric variables are expected to differ substantially between neighbourhoods as well as their

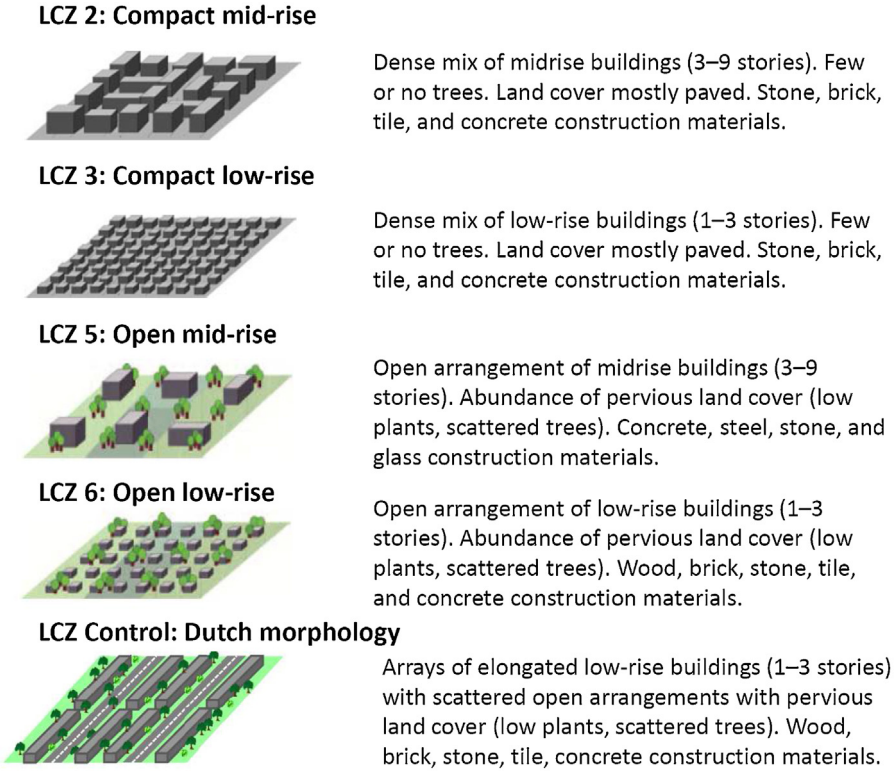

Fig. 1. Overview of local climate zone classifications selected in this study (redrawn and edited from Stewart and Oke, 2012).

land use, anthropogenic activity (commercial, residential, industry) and urban design. To this end we use the classification in so-called Local Climate Zones (LCZ) by Stewart and Oke (2012). District types with low flats and two-storey houses best characterize the typical morphology of Dutch cities and these are selected (see Fig. 1), e.g. compact mid rise (LCZ2), compact low rise (LCZ3), open mid-rise (LCZ5) and open low rise (LCZ6). In addition to these reference LCZ classes, an additional class has been designed that is representing the typical architecture of residential areas in the Netherlands. Dutch residential areas well-known for their relatively long canyons with 2–3 storey buildings, with a front garden, separated by two lane roads. This class will be labelled "LCZcontrol".

3.2. UHI simulations

The Urban Heat Island effects are calculated with the single-column model version of the Weather Research and Forecasting model (WRF, Skamarock et al., 2008) in a similar way as appeared to be fruitful in model simulations for Rotterdam in Theeuwes et al. (2014). These simulations employed the YSU boundary-layer scheme (Hong et al., 2006), the NOAH land-surface model (Ek et al., 2003), the RRTM longwave radiation scheme (Mlawer et al., 1997), the shortwave radiation scheme by Dudhia (1989), and the Kain-Fritsch convection scheme (Kain, 2004). The single-layer urban canopy model (Kusaka et al., 2001) within WRF is designed to quantify the influence of street morphology on the radiation and energy balance of the city. This scheme defines the net albedo of the city by taking into account the reflection of sunlight on the building walls and canyon road. It also takes into account the capturing of outgoing longwave radiation. Further, it calculates thermal storage of heat in buildings, and anthropogenic heat flux. The single-layer urban canopy model requires several parameter values concerning the urban morphology as input. For each local climate zone the values for the model parameters have been defined and these have been summarized in Table 1. The utilized anthropogenic heat flux estimates have been derived for the city of Rotterdam (the Netherlands) with the LUCY model (Lindberg et al., 2013), and these have been applied as forcing in the WRF model. The anthropogenic heat flux amounts to 20 Wm^{-2} for LCZ representing low-rise morphology, and 28 Wm^{-2} for mid-rise morphology. In the current study, the measurement station Cabauw (WMO reference 06348) as operated by the Dutch National Weather Service (Beljaars and Bosveld, 1997) is used as a rural reference. The site is located in a relatively flat and homogeneous grassland area in the Netherlands. The soil consists of clay and water tables are artificially maintained at a high level. Also for this site WRF has been run for the selected heat wave, and the UHI has been determined with respect to this reference. WRF has earlier been extensively validated for Cabauw (Steeneveld et al., 2011b; Kleczek et al., 2014; Sterk et al., 2015; Steele et al., 2015), and therefore we consider a further model validation beyond the scope of the current paper.

Compared to sprawling metropolitan areas around the world, compact Dutch cities are relatively small in terms of surface area. E.g. the largest city Amsterdam has a population of only 838.338 (April 2016) and an surface area of 219 km^2. Therefore, the impact of advection of rural air into the urban areas is not negligible when studying the urban heat island effect. Therefore the model outcome of the run for the rural conditions is used as boundary condition for the runs for the various LCZ. As such, both temperature and humidity are advected into the urban simulations, which depends on the wind speed (that are in general low in heat wave conditions). At each model level a time scale τ is defined that represent the time it takes for rural air to reach the city. The longer it takes the more the atmosphere is able to adjust to the effects of urban morphological parameters. Here we have selected $\Delta X = 10$ km as the distance between the point of interest in the city and the upstream location in the rural surroundings.

We have investigated the weather conditions for the period of 14–19 July 2006, i.e. a heat wave period in the Netherlands. This heat wave was classified to be in the 95 percentile of warmest heatwaves of the 20th century, and as such acts as illustrative example for conditions that are expected to occur more frequently in the future with ongoing climate change. At the same time the human population might become more resilient to urban heat due to adaptation in the future. Bobb et al. (2014) studied the age-stratified mortality rates for 105 U.S. cities during the summers of 1987–2005. They found a significant decline in mortality over this period, particularly for people aged over 75. At the same time

Table 1
Summary of WRF model urban parameter settings used in the numerical experiments.

	LCZ2 Compact mid-rise	LCZ3 Compact low-rise	LCZ5 open mid-rise	LCZ6 Open low-rise	LCZ Control
Fraction Urban (−)	0.85	0.8	0.4	0.35	0.6
Albedo roof (−)	0.08	0.22	0.08	0.22	0.22
Albedo wall (−)	0.25	0.25	0.25	0.3	0.3
Albedo road (−)	0.15	0.3	0.15	0.3	0.3
Heat capacity roof (J/kg/K)	1653300	1596000	1653300	1596000	1596000
Heat capacity wall (J/kg/K)	1418800	1418800	1418800	1007200	1007200
Heat capacity road (J/kg/K)	3910000	2150000	3910000	2150000	3910000
Thermal conductivity roof (W/m/K)	0.55	0.82	0.55	0.82	0.82
Thermal conductivity wall (W/m/K)	0.51	0.51	0.51	0.33	0.38
Thermal conductivity road (W/m/K)	1.2	0.7	1.2	0.7	0.7
H/W (−)	2	0.89	0.5	0.22	0.36
Emissivity roof (−)	0.91	0.9	0.91	0.9	0.9
Emissivity wall(−)	0.9	0.9	0.9	0.9	0.9
Emissivity road (−)	0.94	0.94	0.94	0.94	0.94
Roof height (m)	18	8	18	8	8
Standard deviation roof height (m)	1	1	1	1	1
Roof width (m)	11	10	11	14	10
Road width (m)	9	9	36	36	22
Antr. Heat flux (W/m2)	28	20	28	20	20
Roughness length wall (m)	0.0001	0.0001	0.0001	0.0001	0.0001
Roughness length ground (m)	0.01	0.01	0.01	0.001	0.01
Roughness length roof (m)	0.01	0.01	0.01	0.01	0.01
Roof thickness (m)	0.23	0.08	0.23	0.08	0.08
Wall thickness (m)	0.191	0.191	0.191	0.191	0.191
Road thickness (m)	0.08	0.08	0.08	0.08	0.08
Boundary condition roof, wall, ground	zero-flux	zero-flux	zero-flux	zero-flux	zero-flux

they conclude that even with that increased resilience, substantial risks of heat-related mortality remain. Also Boeckmann and Rohn (2014) conclude that the attribution of health outcomes to heat adaptation remains challenging. While sensitivity to heat appears to be decreasing, the examined studies provide inconclusive evidence on individual planned adaptation measures. Moreover, their study is also inconclusive whether biological adaptation, continuous improvements in healthcare, and to the urban environmental changes others than "adaptation," or different unknown reasons are the basis underneath this mortality decline. However, the uncertainty in future excess mortality due to heat is too high to currently anticipate on in our study at this moment.

3.3. UHI risk quantification

Adverse effects of high temperatures on human population is diverse. While certain effects might be subtle, others result in obvious symptoms such as changes in the cardiovascular system. In more severe cases medical interventions are required, and only the ultimate effect is the premature mortality. Urban heat involves multiple health issues for urban dwellers. Relatively gentle disorders comprises heat syncope or fainting, heat edema or swelling, specifically of the legs, and intermittent cramp as a result of heat-induced hyperventilation. These heat cramps are painful spasms that occurs after exercising in a in a hot environment. Heat exhaustion is a severe and acute illness that may feature nausea, vomiting, weakness and mental status changes. Heat stroke is the most severe and acute heat related condition when the body is unable to dissipate heat (Frumkin, 2002). Also, Goldfarb and Hirsch (2015) hypothesize a relation between urban heat and the prevalence of kidney stones. Moreover, Kaiser et al. (2001) found that mental illness was a possible risk factor for heat-related death during a heat wave in Cincinnati in 1999. It appeared that the risk for dying from heat was highest among people with mental illness who were younger than 65 years. Vanos (2015) reviewed health effects of urban heat and microclimates on children, and she concluded that for adequate play and physical activity, a healthy environment and comfortable microclimatic are needed. Oppressively hot weather and uncomfortable conditions lead to lethargy, decreased work and athletic performance, poor behaviour (Eliasson et al., 2007; Eliasson, 2000; Watkins et al., 2007), and ultimately a deterioration of social and outdoor activity (Johansson and Rohinton, 2006). Recently, Wei et al. (2016) found evidence for enhanced obesity risk and lung inflammation and metabolic disfuction. Ihara et al. (2011) reported that for maximum temperatures above 29.4 °C citizins of Tokyo suffer from restless sleep.

It is rather difficult to quantify the risk of subtle effects and small medical treatments. Therefore in this study we build on the pyramid of health effects and we assume that the mortality that is well documented for a certain effect is also representative for the underlying adverse effects (Fig. 2). Several studies have done the effort to relate mortality to air temperatures. Baccini et al. (2008) found the maximum air temperature as the best indicator for the heat related mortality. On the other hand, Hajat et al. (2002) found the minimum air temperature to be more representative than the maximum air temperature. Overall, the best relation was found between mortality and daily mean air temperatures (Huynen et al. (2001)). To determine the 'extra' risk the UHI cause, we used a linear-threshold model. Because the Netherlands is a small country we did not determine thresholds per region.

We did not have access to mortality data of the Netherlands. According to Huynen et al. (2001) the mortality ratio in the Netherlands is the lowest at a mean daily temperature of 16.5°C.

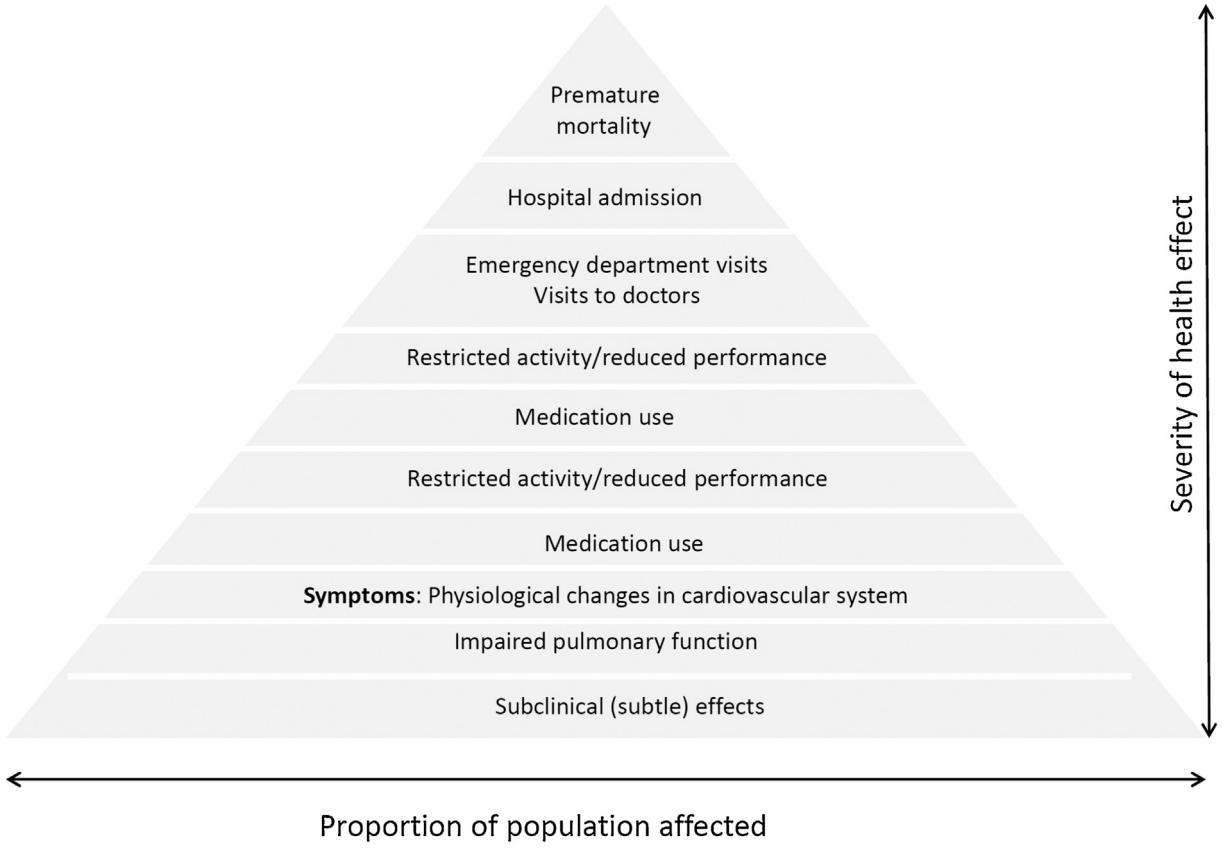

Fig. 2. Pyramid of health effects: proportion of the population affected as function of severity of health effects. Reproduced after WHO (2006).

For temperatures above the optimum, total mortality increased by 2.72% for each degree (Huynen et al., 2001). However, the model for total mortality cannot explain 32% of the mortality during heat waves. Above a temperature of approximately 22 °C the slope of the relationship between temperature and mortality becomes steeper. Assuming that the Dutch wealth and climate is similar to that of the UK, we used the 2.1% (95% CI 1.5–2.7) increase in mortality for every 1 °C rise in temperature above the heat threshold of 21.5 °C (Almeida et al., 2010; Hajat et al., 2014, 2002). See Section 5 for a further discussion of representativeness of the selected temperature metric, and possible adaptation of human population with ongoing climate change.

3.4. Comparison of heat and ozone risks

In this study the impacts of both urban heat and air quality are translated into equal 'health impact units', namely, mortality (see Section 4). The effects of heat and air quality effects (including ozone) form the urban climate index. The assessment methodology follows the excess risk assessment for short term O_3 exposure. To protect our health, vegetation and ecosystems, EU directives set down standards for ozone. In the third daughter directive of CAFE (Clean Air for Europe) a target value, information threshold and alert threshold had been established. The public must be informed/alerted if the ozone concentration exceeds the information/alert threshold. According to the WHO (2008) a threshold (cut-off point) of 70 $\mu g\,m^{-3}$ is set for maximum daily 8-h average. However, Gryparis et al. (2004) showed a conservative threshold of 60 $\mu g\,m^{-3}$ for maximum daily 1-h ozone concentration. Because it is unlikely that the threshold of maximum daily 1-h ozone is lower than maximum daily 8-h, we assume a threshold of 60 $\mu g\,m^{-3}$ for maximum daily 8-h average.

An increase in the 1-h ozone concentration by 10 $\mu g\,m^{-3}$ was associated with a 0.33% (95% confidence interval [CI], 0.17–0.52) increase in the total daily number of deaths (Gryparis et al., 2004). The relative risk of the 8-h ozone concentration appeared to be 0.31% (95% CI, 0.17, 0.52%) per 10 $\mu g\,m^{-3}$ (Gryparis et al., 2004). By using these variables, the excess risk of the different objectives is calculated. The excess risk due to urban heat will also applied to risks associated with health risk at the target value, the information threshold and alert threshold for air quality.

4. Results

4.1. The UHI simulations

Fig. 3 shows the simulated 2-m temperature for 18 and 19 July 2006. These are the last two days of a simulation for 14–19 July 2006. By analysing only the last two days of the simulation, the model has had sufficient time to spin up from its initial state, and has become in a state close to equilibrium (not shown). The model simulation indicates that the rural air temperature reaches its minimum of ~17 °C just before 5.00 UTC, after which the 2-m rapidly increases to reach 28 °C at around 9.00 UTC. The runs for the LCZ follow the same pattern though the temperature increase is less fast compared to the countryside. Between 6.00 and 8.30 UTC the countryside is warmer than the city (see also Theeuwes et al., 2015 for a deeper discussion of the urban cool island effect). In the countryside the maximum temperature is realized at 14.00 UTC, while this appears 1–2 h later in the urban patches. After the evening transition, the cooling in the urban patches starts later, except for the open-low rise local climate zone. The cooling rate in the urban areas is smaller than in the countryside, i.e. most pronounced for compact mid-rise (LCZ2), compact low-rise (LCZ3) and the LCZ control. The lowest minimum temperature is reached in the LCZ open low-rise 19.0 °C, and the highest minimum temperature appears in the compact mid-rise LCZ with a 22.8 °C. A similar pattern appears the following day, which supports the robustness of the model results.

Table 2 summarizes the modelled temperatures in the different LCZ's. During daytime the temperature differences between the city and the countryside are rather limited, irrespective of the LCZ (see also Theeuwes et al., 2015). This is caused by the vigorous turbulence in the convective boundary layer that efficiently mixes away differences in near surface air temperatures that result from the differences in the surface energy balance. During night-time, differences between LCZ temperatures can increase to approximately 5 °C. These differences are caused by the specification of the urban morphology, that result in contrasting heat release due to contrasting heat capacity, heat conductivity, surface emissivity and sky-view factor. The maximum hourly UHI is approximately 6 °C, in correspondence with Heusinkveld et al. (2014).

The highest modelled daily mean temperature on 19 June 2006 amounts to 27.7 °C in LCZ2. The lowest modelled average daily temperature amounts to 25.6 °C in LCZ6. The simulated rural temperature is 24.6 °C, and this temperature is the reference for the

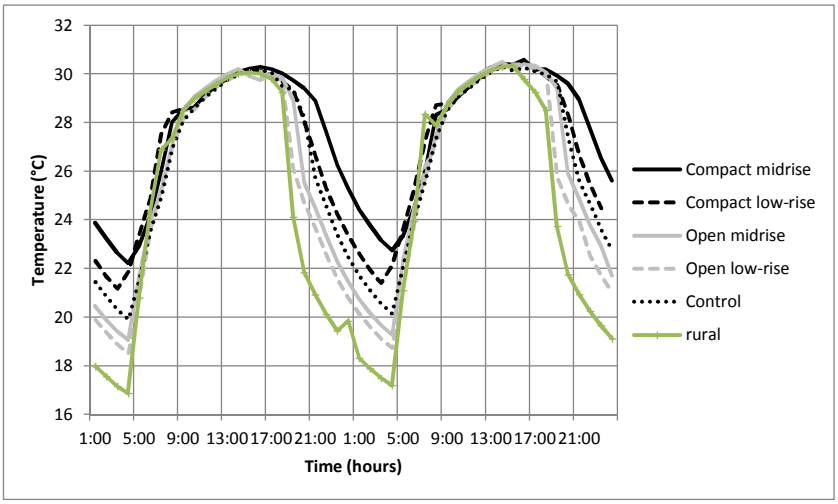

Fig. 3. Model results for 2-m temperature for the selected local climate zones and in the rural area.

Table 2
Urban heat island effect and excess risk (in%) of the local climate zones (LCZ).

	LCZ2	LCZ3	LCZcontrol	LCZ5	LCZ6
daily average temperature (°C)	27.7	27.1	26.4	26.2	25.6
rural temperature (°C)	24.6	24.6	24.6	24.6	24.6
UHI (°C)	3.1	2.5	1.8	1.6	1.0
UHI (°C) (+10% green)	2.8	2.2	1.5	1.2	0.7
UHI (°C) (−10% roof albedo)	3.0	2.4	1.7	1.5	1.0
UHI (°C) (−10% wall albedo)	3.0	2.4	1.8	1.6	1.0
UHI (°C) (−10% road albedo)	3.1	2.5	1.7	1.5	0.9
UHI (°C) (−10 W/m^2 anthropogenic heat)	3.0	2.4	1.7	1.5	0.9
Calculated excess risk of the					
daily average temperature	13.02	11.76	10.29	9.87	8.61
UHI	6.4 (49%)	5.2 (45%)	3.8 (37%)	3.3 (34%)	2.0 (24%)
UHI (+10% green)	5.8 (45%)	4.7 (40%)	3.2 (31%)	2.6 (26%)	1.6 (18%)
UHI (°C) (−10% roof albedo)	6.3 (49%)	5.1 (43%)	3.7 (36%)	3.2 (33%)	2.0 (23%)
UHI (°C) (−10% wall albedo)	6.4 (49%)	5.1 (43%)	3.7 (36%)	3.3 (33%)	2.1 (24%)
UHI (°C) (−10% road albedo)	6.4 (49%)	5.2 (45%)	3.6 (35%)	3.3 (33%)	2.0 (23%)
UHI (°C) (−10 W/m^2 anthropogenic heat)	6.3 (48%)	5.0 (43%)	3.6 (35%)	3.1 (32%)	1.9 (22%)

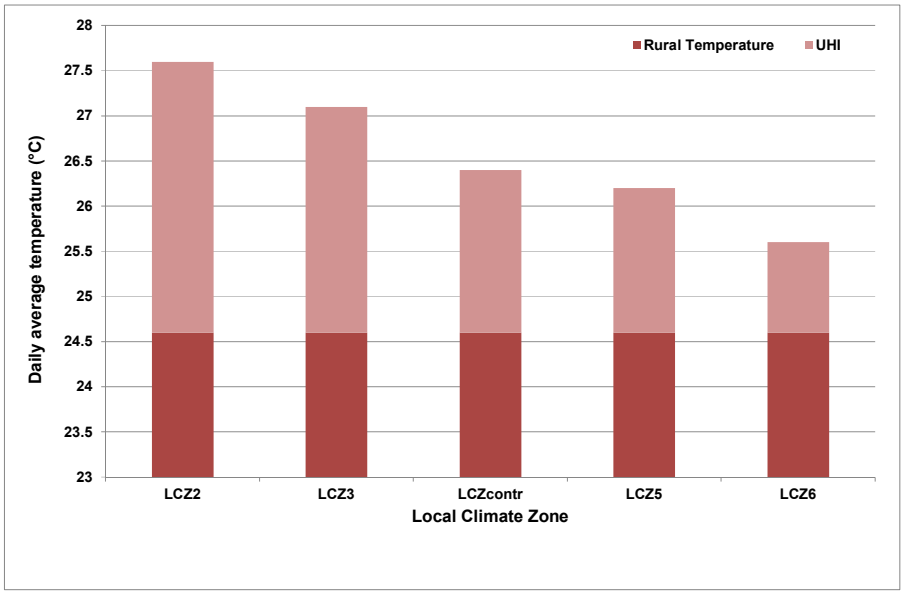

Fig. 4. The simulated daily average temperature on 19 July 2006, subdivided in rural temperature and urban heat island effect.

heat index in the countryside. The daily mean UHI amounts to 3.1 °C and 2.5 °C in LCZ2 and LCZ 3 respectively. In the relatively less densely built LCZ 5 and LCZ6, the UHI amounts to 1.6 °C and 1.0 °C respectively (Table 2, Fig. 4).

To show the effectiveness of adaptive measures in the different LCZs, the modelled daily mean temperature for varying anthropogenic heat flux, green fraction, wall, roof and road albedo, is presented in Fig. 5. The influence of these parameters on the daily mean temperature is tapering, the relationship at varying parameter values is often non-linear. The difference between 0 and 100% green is a maximum of 3.3 °C (LCZ5) and a minimum of 2.5 °C (LCZ6). It is therefore the most effective adaptive measure from the ones studied here. Also Steeneveld et al. (2011a) and Heusinkveld et al. (2014) found this high sensitivity of the UHI to the green vegetation index in earlier studies for the Netherlands. On one hand the evapotranspiration by green vegetation results in a smaller amount of surface energy being available for the sensible heat flux and this results in a smaller daytime heating. Also, at night a green vegetation provides a high sky view factor combined with an efficient isolation from the subsoil, and therefore results in an efficient cooling.

A reduction in anthropogenic heat, from 55 to 0 Wm^{-2} can diminish the temperature with 0.8 °C in LCZ3. In LCZ5, LCZ 6, and LCZcontrol reducing the anthropogenic heat production also weakens the UHI, though slightly less efficient than for the LCZ above. Considering albedo in the city's design we find that the more compact and less green local climate zones (LCZ2 and LCZ3) the maximum increase in wall albedo appreciates the strongest temperature reduction compared to the other LCZs. An increase in roof albedo is most effective in LCZ2 and least effective in LCZ6. The sensitivity to road albedo is rather limited, likely due to its rather deep positioning in the canyon. The influence of road albedo is the highest in LCZcontrol. This is due to the fact that the roads are wider in these LCZs compared to the roads in LCZ2 and LCZ3. The model results are more sensitive to the wall albedo, particularly for LCZ2 and LCZ3, where 0.5 °C temperature reduction can be achieved by increasing the albedo from 6% to 82%. It should be noted that the model does not take into account the aging of interventions, i.e. the albedo remains constant in the simulations, while in reality deposition of air pollution will reduce the albedo after the intervention. Also note that the in these experiments the impact of possible interventions has been modelled assuming that the other parameters for the city remained constant. For example, variations in roof albedo for a certain LCZ have been estimated using the default surface green fraction for that LCZ. This implies that adjusting the albedo

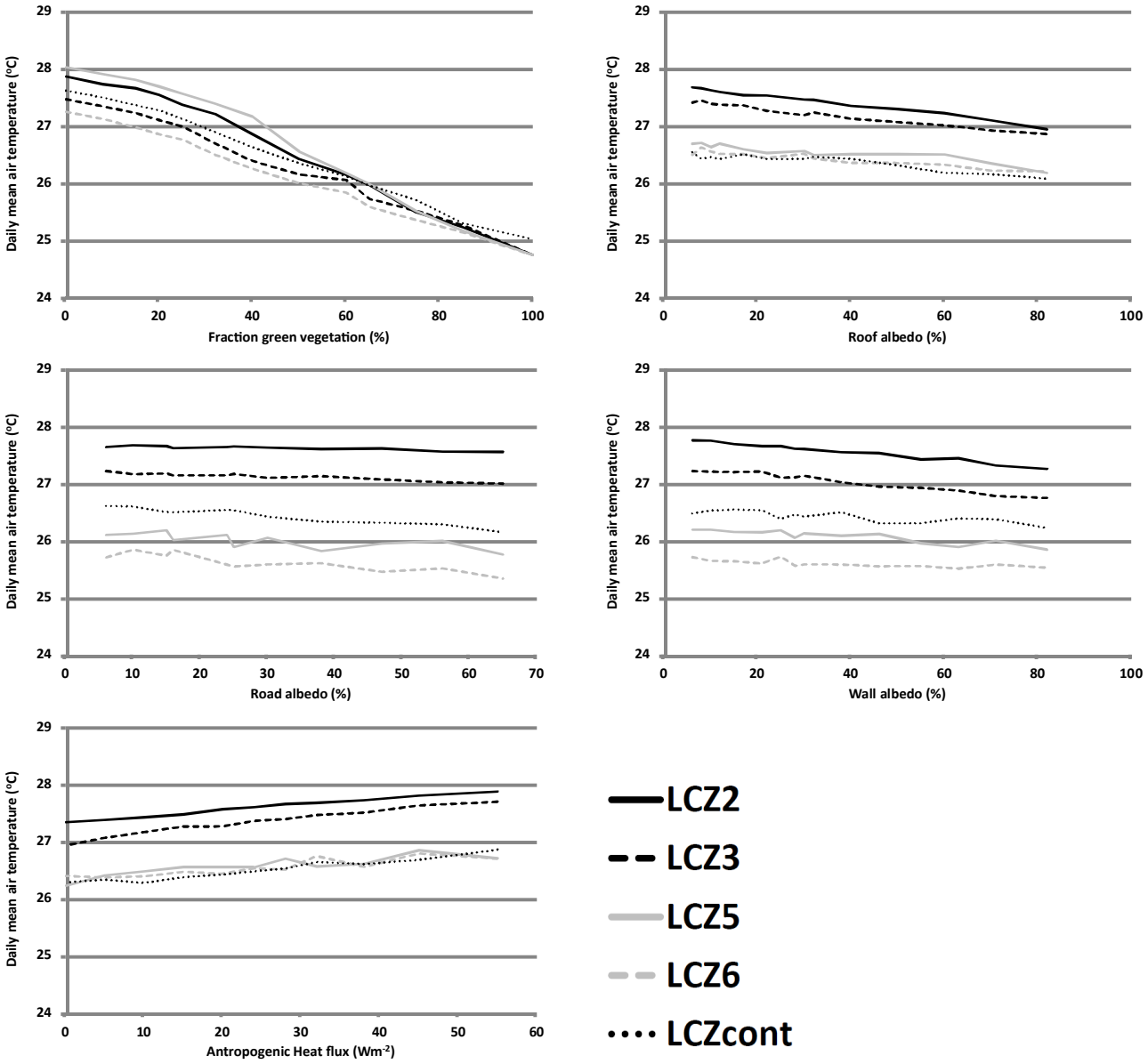

Fig. 5. The modelled daily average temperature for 19 July 2006 as function of roof albedo (a), road albedo (b), wall albedo (c), green vegetation fraction (d) and anthropogenic heat production (e) for several local climate zones.

has more impact in an LCZ with a low surface green fraction than in an LCZ with a high green fraction.

4.2. The health risk of the UHI

To quantify the excess risk due to the UHI, we assume that mortality increases with 2.1% per degree Celsius above a daily average temperature of 21.5 °C (see Section 3.3). To assess the excess risk of the UHI of the LCZs, the risk due to the UHI is determined corresponding to the excess risk of the target objective, information and alert threshold as was already formulated for air quality (Table 2). According to this table the excess risk of the UHI of LCZ5, LCZ6 and LCZcontrol are higher than the excess risk of the target value of ozone (shown in Table 3). The excess risk of the UHI in LCZ3 exceeds the excess risk of the information threshold. In LCZ2 the excess risk is even higher than the excess risks of the alert threshold. Moreover we find that 10% extra green area surface will reduce the excess risk in LCZ2 to a level below the excess risk of the alert threshold. In LCZ6 the excess risk of the UHI contribution decreases to 1.6 with 10% extra green surface vegetation cover.

Next we present a numerical example that illustrates the application of the urban climate index. The heat index can be relatively easily calculated as the 24-h mean value of the UHI in the neighbourhood divided by the maximum 24-h mean UHI, thus $UHI_{day,neigh}/UHI_{day,max}$. The maximum UHI_{day} has been estimated by the simulated heat wave, and appeared to be 3.3 °C from the WRF model simulations. Thus the heat index has been normalised with the maximum daily mean UHI from the model results. Table 4 presents a numerical example for the calculation of the risk due to urban heat, i.e. the risk above the already present risk in the countryside. Since the risk in countryside is solely governed by meteorological factors and can as such not be influenced by interventions, the risk due to the (adaptable) urban morphology is quantified separately. The total risk is therefore composed of a rural and an urban contribution. The risk by the rural temperature amounts to 6.3% ((24,6 °C (rural mean temperature) – 21.5 °C (threshold)) * 2.1%). The extra contribution due to the UHI may

Table 3
The excess risk of the target objective, information and alert threshold and the corresponding daily mean UHI.

Objectives	Parameter	Concentration (ug/m3)	Excess risk (%)	Corresponding UHI (°C)
target value	maximum daily 8 h mean	120	1.86	0.89
information threshold	1 h average	180	3.96	1.89
alert threshold	1 h average	240	5.94	2.83

Table 4
Overview of the quantification of health risk (%) due to heat, separated by rural and urban sites.

Temperature (°C)	Total heat risk (rural + urban) (%)	UHI (°C)	Extra risk due to UHI (%)
21.5	0	0	0
22	1.05	0	0
22.5	2.1	0	0
23	3.15	0	0
23.5	4.2	0	0
24	5.25	0	0
24.5	6.3	0	0
25	7.35	0.4	0.84
25.5	8.4	0.9	1.89
26	9.45	1.4	2.94
26.5	10.5	1.9	3.99
27	11.55	2.4	5.04
27.5	12.6	2.9	6.09
28	13.65	3.4	7.14

Table 5
Overview of heat index categorisations.

Category	Heat index	
0	0 -0.3	Comfortable
I.	0.3 - 0.6	Acceptable
II.	0.6 -0.9	Risk
III.	0.9- 1.0	Unacceptable

exceed 7% (3.3 °C * 2.1%). This means that risk of mortality during a heat wave can be doubled by the UHI. Table 5 presents the health risk due to high temperatures after categorization into classes that corresponds to the air quality threshold values.

Table 2 illustrates the influence of urban design interventions as discussed in Section 4.1 on excess mortality risk. In the reference conditions, the excess risk amounts to 13% for LCZ and deacreses to 8.6% for LCZ6. The UHI contribution, i.e. the part that is partly regulated by design intervention, appears to 6.4% in LCZ and decreases to 2.0% for LCZ6. The table also reveals that the urban contribution to this excess risk is about 50% in LCZ2, but only 25% in LCZ6, with the other LCZs in an intermediate position.

The proposed intervention measures are partly successful in reducing the excess risk. The enhanced green vegetation reduces the excess risk by 0.4-0.6% within the different LCZ. We also find that the excess risk decline by reducing the albedo of the building material has only a marginal effect. On the other hand, a reduction of the anthropogenic heat projection might allow for a further 0.2% excess risk reduction.

4.3. Air quality index

The air quality index in this study is based on both the particulate matter species group PM10 (Effect_PM10) and the ozone effect (Effect_O3), i.e.

$$\text{AQ-index} = \{\text{Effect\_PM10} + \text{Effect\_O3}\} * \text{normalisationfactor}.$$

Table 6
Overview of air quality index categorisations.

Category	AQ index	
0	0 - 0.1	Comfortable
I.	0.1 -0.2	Acceptable
II.	0.2 - 0.4	Risk
III.	0.4 - 0.6	Unacceptable
IV	0.6- 1.0	Urgent

Herein the normalisation factor equals 1/12, since the maximum excess risk according to our method amounts to 12 (ozone = 240 $\mu g\,m^{-3}$ and PM10 = 150 $\mu g\,m^{-3}$).

The AQ-index can be rewritten to

$$\text{AQ-index} = \{([PM_{10}]_{\text{dailymean}} - \text{threshold\_PM}_{10}) * (RR\_PM_{10\text{dailymean}} + (([NO_2]\text{jm} - \text{threshold\_NO}_2) * (cRR\_NO_2\text{-jm}))) + ([O_3]8\,\text{h} - \text{threshold\_O}_3) * RR\_O_3\text{–}8\,\text{h}\} * \text{normalisationfactor}.$$

Hence,

$$\text{AQ-index} = \{([PM10]_{\text{dailymean}} - 10\,\mu g/m3) * (0.042 + ([NO_2]\text{jm} - 21\,\mu g/m3) * 0.015) + ([O_3]8\,\text{h} - 50\,\mu g/m3) * 0.031\} * 0.083.$$

Herein, threshold_PM10 is the daily mean PM10 concentration that does not contribute to enhanced adverse health effects (here 10 $\mu g\,m^{-3}$ as 'natural background'), RR_PM10_{day} indicates the relative risk (per 1 $\mu g/m3$) of a daily mean PM10 concentration that proceeds for several days, which is taken as 0.042% (Touloumi et al., 2004), threshold_NO_2: denotes the yearly mean NO_2 concentration that does not contribute to enhanced adverse health effects (here 21 $\mu g\,m^{-3}$ as 'natural background' for Belgium and the Netherlands has been employed following CBS et al., 2013). In addition, cRR_NO_2-jm denotes a correction of relative risk (per 1 $\mu g\,m^{-3}$) of the daily mean PM10 concentration as a result of the yearly mean NO_2 concentration (here 0.015% is taken), and threshold_O_3 denotes the 8 h mean O_3 concentration that does not contribute to enhanced adverse health effects, and has been found 50 $\mu g\,m^{-3}$ in Powell et al. (2012). Finally RR_O_3–8 h indicates the relative risk (per 1 $\mu g\,m^{-3}$) of 8-h O_3 concentrations (determined at 0.033%).

For practical use, the AQ index values have been grouped in five classes (Table 6), that express the excess risk with respect to the maximum excess risk possible in this study. Class 0 contains an AQ index of 0–0.1 and this is interpreted as comfortable. Class I (acceptable) indicates an AQ index of 0.1–0.2, while risk starts to appear if the AQ index amounts to 0.2–0.4. The air quality appears to be unacceptable for AQ index in the range 0.4–0.6, while air quality problems becomes urgent for AQ index >0.6.

4.4. A new urban climate index

The UC-index is meant to be an unambiguous (objective) measure, which is intended to indicate the extent of a heat problem in a neighbourhood. The UC-index is defined here as a local risk poten-

Table 7
Overview of combined heat and air quality index in the urban climate index.

Urban Climate Index

Air Quality Index \ Heat Index	0	0.05	0.1	0.15	0.2	0.25	0.3	0.35	0.4	0.45	0.5	0.55	0.6	0.65	0.7	0.75	0.8	0.85	0.9	0.95	1
1	100	105	110	115	120	125	130	135	140	145	150	155	160	165	170	175	180	185	190	195	200
0.95	95	100	105	110	115	120	125	130	135	140	145	150	155	160	165	170	175	180	185	190	195
0.9	90	95	100	105	110	115	120	125	130	135	140	145	150	155	160	165	170	175	180	185	190
0.85	85	90	95	100	105	110	115	120	125	130	135	140	145	150	155	160	165	170	175	180	185
0.8	80	85	90	95	100	105	110	115	120	125	130	135	140	145	150	155	160	165	170	175	180
0.75	75	80	85	90	95	100	105	110	115	120	125	130	135	140	145	150	155	160	165	170	175
0.7	70	75	80	85	90	95	100	105	110	115	120	125	130	135	140	145	150	155	160	165	170
0.65	65	70	75	80	85	90	95	100	105	110	115	120	125	130	135	140	145	150	155	160	165
0.6	60	65	70	75	80	85	90	95	100	105	110	115	120	125	130	135	140	145	150	155	160
0.55	55	60	65	70	75	80	85	90	95	100	105	110	115	120	125	130	135	140	145	150	155
0.5	50	55	60	65	70	75	80	85	90	95	100	105	110	115	120	125	130	135	140	145	150
0.45	45	50	55	60	65	70	75	80	85	90	95	100	105	110	115	120	125	130	135	140	145
0.4	40	45	50	55	60	65	70	75	80	85	90	95	100	105	110	115	120	125	130	135	140
0.35	35	40	45	50	55	60	65	70	75	80	85	90	95	100	105	110	115	120	125	130	135
0.3	30	35	40	45	50	55	60	65	70	75	80	85	90	95	100	105	110	115	120	125	130
0.25	25	30	35	40	45	50	55	60	65	70	75	80	85	90	95	100	105	110	115	120	125
0.2	20	25	30	35	40	45	50	55	60	65	70	75	80	85	90	95	100	105	110	115	120
0.15	15	20	25	30	35	40	45	50	55	60	65	70	75	80	85	90	95	100	105	110	115
0.1	10	15	20	25	30	35	40	45	50	55	60	65	70	75	80	85	90	95	100	105	110
0.05	5	10	15	20	25	30	35	40	45	50	55	60	65	70	75	80	85	90	95	100	105
0	0	5	10	15	20	25	30	35	40	45	50	55	60	65	70	75	80	85	90	95	100

tial, which can be assessed as a quality of the environment. For the overall evaluation is important to take account of the heat and AQ-index in the proper ratio. The degree of harmfulness of heat and air pollution, can be based on available scientific literature. Research in England on the 2003 heatwave shows that 20–40% of the increased mortality is caused by air pollution (O_3 and PM10). This is in accordance with investigations of the 2003 heat wave in Netherlands. Research by the Euroheat project shows that a major contributor to the increased mortality during heat waves, comes from PM10 (~30%) and ozone (~15–25%). The relative risks were made when the heat index and AQ-index and have a range in accordance with the above-mentioned literature. Here the simulated heat wave shows that the extra risk of heat is a maximum of approximately 13.6% and by air pollution 12%. For heat, we assume the additional impact due to urban environments relative to the rural reference. From the current study the overall risk for these rural reference is 6.5%. Finally, the urban climate – index is calculated as follows: UC-index = (Heat-index + AQ-index) * 100 (Table 7).

4.5. An application of the new urban climate index

In this section we present an example of the application of the urban climate index. This is done for the Dampoort neighbourhood in Ghent (Belgium). Ghent is a midsize city (251.133 inhabitants, January 2014) located in the west of Belgium (51° 3′ N, 3° 42′ E). Fig. 6 shows the Dampoort neighbourhood. This neighbourhood is suitable for illustrating the UCAM methodology because it is located in the inner city of Ghent, and because it is characterised by a high degree of built up and impervious surfaces, as well as by the presence of my sources of air pollution. Moreover, the green vegetation fraction amounts to 18%, and the Dampoort was classified to be most closely related to Local Climate Zone 3. The neighbourhood is characterised by clear differences in green vegetation cover, i.e. the southern part of Dampoort is covered with green vegetation for 32% while this is only 13% for its northern counterpart (Table 8).

Table 7 illustrates the application of the UCAM method for the selected heat wave in 2006. The northern part of Dampoort is rather vulnerable to urban heat. Its UHI amounts to 2.7 °C, which results in an heat index of 0.81 (the $UHI_{day}/UHM_{day,max}$ = 2.7/3.3). In the rural area the excess mortality risk amounts to 6.5% ((24.6 °C–21.5 °C)*2.1%), while this amounts to 12.2% ((27.3 °C–21.5 °C)*2.1%). Consequently, the enhancement of the excess risk for the northern part of the neighbourhood appears to be 87% (12.2%/6.5%). Hence in this case the neighbourhood's urban heat problem reaches category IV, and this risk is comparable to the alarm threshold for ozone. Fortunately the high urban contribution also indicates that interventions in the urban morphology might assist in ameliorating the neighbourhood's environmental quality.

In the southern part of Dampoort, the heat index reaches category III, although this still means that this is comparable to exceeding the information threshold for ozone. The modelled UHI amounts to 2.1 °C, which results in an heat index of 0.64, and an urban contribution of 67%. Overall the heat analysis indicates the that health risks are substantially raised during heat waves. This leads to unacceptable human-induced health risks that are comparable to risks that represent the alarm threshold for ozone.

Table 7 also shows the contributions of air quality to the environmental quality. The air quality index amounts to 0.35, 0.41, and 0.39 for the rural background, the northern and southern part of Dampoort respectively, and these correspond to categories II, III, and II respectively. The results for the air quality index vary marginally, which is explained by the relatively large contribution of air pollution that originates from the rural surroundings (regional contribution). Although the local contribution of PM10 exceeds the yearly mean contribution this aspect is small compared to the large scale regional contribution. Therefore the urban contribution to air quality appeared to be only 17 and 12% for the two parts of Dampoort respectively. This assessment provides a point of departure for possible interventions that ameliorate the urban environmental quality.

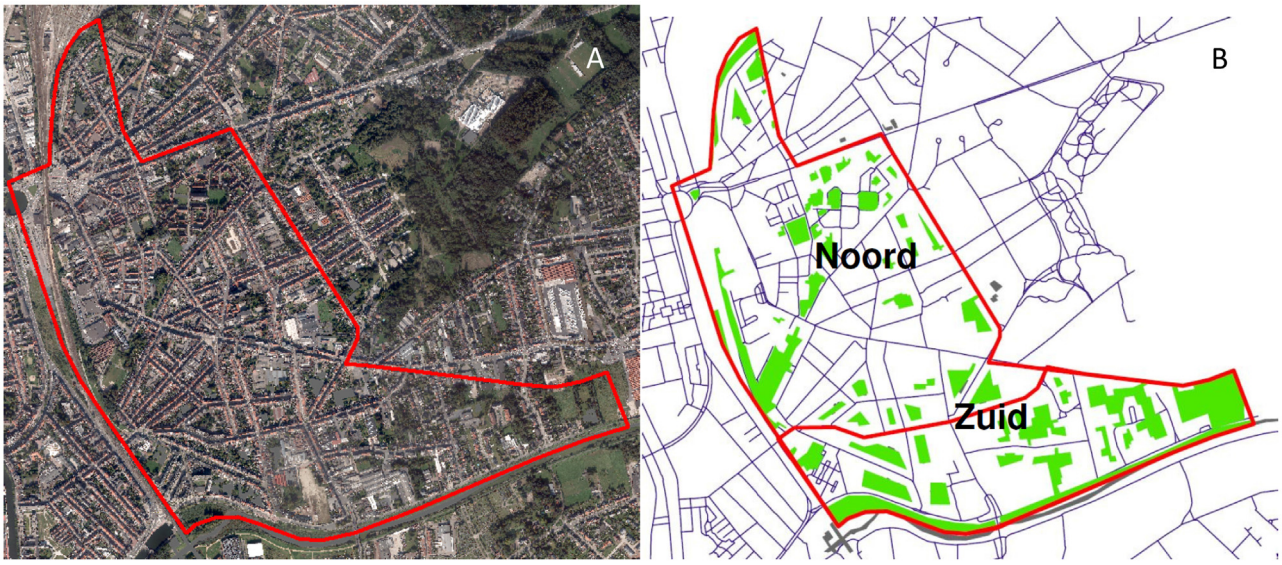

Fig. 6. Land use map of the Dampoort neighbourhood (red contour) in Ghent (Belgium) (panel a). Illustration of the green fraction in the northern and southern parts Dampoort (panel b). (For interpretation of the references to colour in this figure legend, the reader is referred to the web version of this article.)

5. Discussion

In this paper we quantified the urban heat island of different urban areas by simulating a heat wave using the Weather Research and Forecasting model. Results of the heat wave simulation are linked to relative risks of exposure to high temperatures to determine the excess risk of the UHI. Moreover, the excess risks of the LCZs are compared to the excess risks of the target value, information threshold and alert threshold of exposure to ozone. Results of this study show that the excess risk in all LCZs (default settings) exceeds the excess risk that is similar to the target value of ozone. In LCZ2 and LCZ3 the excess risk even exceeds the risks of the alert threshold and information threshold of ozone, respectively. Results further show that certain measures (physical interventions in built area) do have a positive effect and contribute to city adaptation to urban heat, thereby reducing potential health risks.

A few studies of the effects of exposure to high temperatures have taken the variation of temperatures in cities into account. Vandentorren et al. (2006) showed that the temperature index of the urban area significantly increased the risk of premature mortality during the 2003 heat wave in France. Smoyer (1998) indicated that heat-related mortality rates during heat waves were generally higher in the warmer areas of St. Louis (Missouri) compared to the cooler parts. However, most studies on the effects of hot weather attribute temperatures to an entire region based on a small number of meteorological stations often located at airports (Smargiassi et al., 2009). In this study we were able to attribute temperatures to neighbourhoods.

In addition, as mentioned in Section 3.3, the literature indicates quite some variety on what is the leading temperature that relates best to mortality, i.e. daily mean temperature, maximum temperature or minimum temperature. Maximum temperature as indicator would imply that the urban contribution to mortality would be rather small, since the urban heat island effect is then smaller than in the evening or at night. An apparent temperature with a physically sound background, i.e. based on the modelling of the human energy balance with temperature, humidity, wind speed and radiation as input, is expected to relate best to mortality rates, e.g. the physiological equivalent temperature, or the universal thermal comfort index (UTCI). Results by Morabito et al. (2014) found enhanced correspondence of UTCI as mortality predictor than other temperature metrics. On the other hand, Urban and Kyselý (2014) studied the mortality due to cardiovascular diseases with respect to daily mean air temperature, UTCI, apparent temperature and physiologically equivalent temperature (PET). They found similar heat effects on mortality for air temperature and the examined thermal indices, while for cold-related mortality the UTCI and PET showed to be preferred indices over air temperature. Given the focus of our paper on heat related mortality, and the uncertainties summarized above, and since UTCI (and PET) estimation from routine weather data is not straightforward, daily mean air temperature as predictor for excess mortality appears defendable.

It is important to note that the applicability of the method utilizing the relative risk values and threshold values is limited to North Western Europe. The strategy behind the risk quantification is thought to be applicable in a broader scope if the risk and threshold values are known for other the regions. Also, the risk and threshold values have been based on data gathered in the past. First one has to realize that risk and threshold values might be re-determined in future studies and this may reduce the uncertainty. In addition, the relative risk values may vary in time due to several aspects, i.e. composition of the pollutant (i.e. PM10 also contains components that are less dangerous for the human health, e.g. sea salt). Finally, we realize that in this study the relative health risks have been quantified for each LCZ, but for air quality this has not been done so far. This depends much on the local situation. Although the monitoring of traffic related influence on air quality is well developed, the translation into short term health effects during atmospheric conditions during heat waves has hardly been investigated. We recommend this as a next step in the refinement of the UCAM methodology.

Specific components within PM10, like sooth (EC), ultrafine particles, etc, are expected to have a stronger relation to health effects, and are higher in urban areas, but contribute small to the mass concentration of PM10. This implies to search for a stronger indicator for urban AQ than PM10, which can be adopted in the UCAM-method.

Moreover, this study shows that the air temperatures can vary greatly within a city. This illustrates that for the assessment of health risk due to urban air temperature, meteorological stations

Table 8
Overview of urban environmental quality assessment parameters for the Dampoort neighbourhood in Ghent (Belgium) for the heat wave in 2006.

Area	LCZ	% Green	Mean Temp (°C)	UHI (°C)	Heat index (–)	Category Heat index	PM10 yearly mean conc (μ/m3)	PM10 daily mean conc (μ/m3)	NO2 yearly mean conc (μ/m3)	O3 8 h concentration (μ/m3)	Air Quality index (–)	Category AQ index	Urban climate index (–)	Neighborhood Contribution Heat	Neighborhood Contribution Air Quality
Rural			24.6		0	0	29	46	27	121	0.35	II	35	0	0
Dampoort North	3	13	27.3	2.7	0.818182	IV	32	50	35	121	0.41	III	121	86%	17%
Dampoort South	3	32	26.7	2.1	0.636364	III	31	49	33	121	0.39	III	102	67%	12%

should also be located inside urban areas. Applying temperature observations from routine WMO weather stations will result in an underestimation of the estimated heat load. Alternatively, air temperature data as recorded by hobby meteorologists offer the opportunity to refine the knowledge of local urban temperature fields (Steeneveld et al., 2011a; Bell et al., 2015). Nowadays multiple online networks are available to perform the observations, and to disclose them to the general as well as to the scientific audience. For example, the websites www.wunderground.com and www.netatmo.com allows for a nearly realtime monitoring of urban weather. Moreover, both the British and Dutch national weather services have taken the initiative to collect these data and evaluate their additional value for understanding urban weather and climate, and to improve the fine scale weather forecasts (see e.g. http://wow.metoffice.gov.uk/andwow.knmi.nl). In case reliable urban meteorological observations are missing, the presented UCAM method can be used to fill this gap.

6. Conclusion

Cities are subject to the urban heat island effect and high pollution concentration. Both deteriorate human health of their inhabitants. This study developed a metric that accounts for the combined health effect of high temperatures during heatwaves as well as by high pollution concentrations. Thereto the relative health risk, as expressed by increase in mortality, due to temperature has been expressed in an analogous way as was already available for air quality, i.e. ozone. Information and alert values for air quality induce a certain relative risk and these specific risk values have been applied to excess mortality due to heat. Hence, the health risk due to high temperatures can inversely be quantified and compared to air quality induced health risks. Thereto the urban climate index that combines the health risk of both environmental hazards is developed. Finally, the application of the urban climate index is illustrated for an urban planning assignment in Ghent (Belgium).

Acknowledgements

The authors acknowledge the financial support from the “Climate Changes Spatial Planning” Valorius scheme, the Dutch ministry of Infrastructure and Environment, and the city of Ghent (Belgium). Moreover we thank Sytse Koopmans (Wageningen University), Jimme Zoete (Witteveen+Bos), Bart van den Hurk, Erik Min, Dirk Wolters and Henk Eskes (KNMI) for their contributions and suggestions.

References

Almeida, S.P., Casimiro, E., Calheiros, J., 2010. Effects of apparent temperature on daily mortality in Lisbon and Oporto, Portugal. Environ. Health 9, 12.
Analitis, A., Katsouyanni, K., Biggeri, A., Baccini, M., Forsberg, B., Bisanti, L., Kirchmayer, U., Ballester, F., Cadum, E., Goodman, P.G., Hojs, A., Sunyer, J., Tiittanen, P., Michelozzi, P., 2008. Effects of cold weather on mortality: results from 15 European cities within the PHEWE project. Am. J. Epidemol. 168, 1397–1408.
Anderson, B.G., Bell, M., 2009. Weather-related mortality: how heat, cold, and heat waves affect mortality in the United States. Epidemiology 20, 205–213.
Böcker, L., Thorsson, S., 2014. Integrated weather effects on cycling shares, frequencies and durations in Rotterdam, The Netherlands. Weather Clim. Soc. 6, 468–481.
Baccini, M., Biggeri, A., Accetta, G., Kosatsky, T., Katsouyanni, K., Analitis, A., Anderson, H.R., Bisanti, L., D'Ippoliti, D., Danova, J., Forsberg, B., Medina, S., Paldy, A., Rabczenko, D., Schindler, C., Michelozzi, P., 2008. Heat effects on mortality in 15 European cities. Epidemiology 19, 711–719.
Beljaars, A., Bosveld, F., 1997. Cabauw Data for the Validation of Land Surface Parameterization Schemes. J. Climate 10, 1172–1193.
Bell, S., Cornford, D., Bastin, L., 2015. How good are citizen weather stations? Addressing a biased opinion. Weather 70, 75–84.
Bobb, J.F., Peng, R.D., Bell, M.L., Dominici, F., 2014. Heat-related mortality and adaptation to heat in the United States. Environ. Health Perspect. 122, 811–816.

Boeckmann, M., Rohn, 2014. Is planned adaptation to heat reducing heat-related mortality and illness? A systematic review. BMC Pub. Health 14 (1112), http://dx.doi.org/10.1186/1471-2458-14-1112.
Bohnenstengel, S.I., co-authors, 2015. Meteorology, air quality, and health in London: the ClearfLo project. Bull. Am. Meteorol. Soc. 96, 779–804.
Budd, G.M., 2001. Assessment of thermal stress – The essentials. J. Therm. Biol. 26, 371–374.
CBS, PBL, Wageningen U.R., 2013. Stikstofoxiden in lucht, 1990–2012 (indicator 0493, versie 07, 31 oktober 2013). www.compendiumvoordeleefomgeving.nl. CBS, Den Haag; Planbureau voor de Leefomgeving, Den Haag/Bilthoven en Wageningen UR, Wageningen. In Dutch.
Conti, S., Meli, P., Minelli, G., Solimini, R., Toccaceli, V., Vichi, M., Beltrano, C., Perini, L., 2005. Epidemiologic study of mortality during the Summer 2003 heat wave in Italy. Environ. Res. 98, 390–399.
Curriero, F.C., Heiner, K.S., Samet, J.M., Zeger, S.L., Strug, L., Patz, J.A., 2002. Temperature and mortality in 11 cities of the Eastern United States. Am. J. Epidemiol. 155, 80–87.
Dijst, M., 2013. Space-time integration in a dynamic urbanizing world: current status and future prospects in geography and GIScience: space-time integration in geography and GIScience. Ann. Assoc. Am. Geogr. 103, 1058–1061.
Dudhia, J., 1989. Numerical study of convection observed during the Winter Monsoon Experiment using a mesoscale two–dimensional model. J. Atmos. Sci. 46, 3077–3107.
EPA, 2015. National Ambient Air Quality Standards (NAAQS), Online available via: http://www3. epa.gov/ttn/naaqs/criteria.html.
Ek, M.B., Mitchell, K.E., Lin, Y., Rogers, E., Grunmann, P., Koren, V., Gayno, G., Tarpley, J.D., 2003. Implementation of Noah land surface model advances in the National Centers for Environmental Prediction operational mesoscale Eta model. J. Geophys. Res. 108, 8851, http://dx.doi.org/10.1029/2002JD003296.
Eliasson, I., Knez, I., Westerberg, U., Thorsson, S., Lindberg, F., 2007. Climate and behaviour in a Nordic city. Landsc. Urban Plan. 82, 72–84.
Eliasson, I., 2000. The use of climate knowledge in urban planning. Landsc. Urban Plan. 48, 31–44.
Frumkin, H., 2002. Urban sprawl and public health. Public Health Rep. 117, 201–217.
Garssen, J., Harmsen, C., De Beer, J., 2005. The effect of the summer 2003 heat wave on mortality in the Netherlands. Euro Surveill. 10, 165–168.
Goldfarb, D.S., Hirsch, J., 2015. Hypothesis: urbanization and exposure to urban heat islands contribute to increasing prevalence of kidney stones. Med. Hypotheses 85, 953–957.
Gryparis, A., Forsberg, B., Katsouyanni, K., Analitis, A., Touloumi, G., Schwartz, J., Samoli, E., Medina, S., Anderson, Maria Niciu, E., Kriz, B., Kosnik, M., Skorkovsky, J., Vonk, JM, Dörtbudak, Z., 2004. Acute effects of ozone on mortality from the air pollution and health: a European approach project. Am. J. Respir. Crit. Care Med. 170, 1080–1087.
Höppe, P., 1999. The physiological equivalent temperature – a universal index for the biometeorological assessment of the thermal environment. Int. J. Biometeorol. 43, 71–75.
Hajat, S., Kovats, R.S., Atkinson, R.W., Haines, A., 2002. Impact of hot temperatures on death in London: a time series approach. J. Epidemiol. Community Health 56, 367–372.
Hajat, S., Vardoulakis, S., Heaviside, C., Eggen, B., 2014. Climate change effects on human health: projections of temperature-related mortality for the UK during the 2020, 2050s and 2080. J. Epidemiol. Community Health 68, 641–648, http://dx.doi.org/10.1136/jech-2013-202449.
Hanna, E.G., Kjellstrom, T., Bennett, C., Dear, K., 2011. Climate change and rising heat: population health implications for working people in Australia. Asia Pac. J. Public Health 23, 14S–26S.
Helbich, M., Böcker, L., Dijst, M., 2014. Geographic heterogeneity in cycling under various weather conditions: evidence from Greater Rotterdam. J. Transp. Geogr. 38, 38–47.
Heusinkveld, B.G., Steeneveld, G.J., van Hove, L.W.A., Jacobs, C.M.J., Holtslag, A.A.M., 2014. Spatial variability of the Rotterdam urban heat island as influenced by urban land use. J. Geophys. Res. Atmos. 119, 677–692.
Hong, S.Y., Noh, Y., Dudhia, J., 2006. A new vertical diffusion package with an explicit treatment of entrainment processes. The journal abbreviation is M̈on. Wea Rev. (Monthly Weather Review) 134, 2318–2341.
Huynen, M.M., Martens, P., Schram, D., Weijenberg, M.P., Kunst, A.E., 2001. The impact of heat waves and cold spells on mortality rates in the Dutch population. Environ. Health Perspect. 109, 463.
Ihara, T., Kusaka, H., Hara, M., Matsuhashi, R., Yoshida, Y., 2011. Estimation of mild health disorder caused by urban air temperature increase with midpoint-type impact assessment methodology. J. Environ. Eng. 76, 459–467.
Jendritzky, G., De Dear, R., Havenith, G., 2012. UTCI – why another thermal index? Int. J. Biometeor. 56, 421–428.
Johansson, E., Rohinton, E., 2006. The influence of urban design on outdoor thermal comfort in the hot humid city of Colombo, Sri Lanka. Int. J. Biometeorol. 51, 119–133.
Kain, J.S., 2004. The Kain–Fritsch convective parameterization: an update. J. Appl. Meteorol. 43, 170–181.
Kaiser, R., Rubin, C.H., Henderson, A.K., Wolfe, M.I., Kieszak, S., Parrott, C.L., Adcock, M., 2001. Heat-related death and mental illness during the 1999 Cincinnati heat wave. Am. J. Forensic Med. Pathol. 22, 303–307.
Kleczek, M.A., Steeneveld, G.J., Holtslag, A.A.M., 2014. Evaluation of the Weather Research and Forecasting mesoscale model for GABLS3: Impact of boundary-layer schemes: boundary conditions and spin-up. Bound.-Layer Meteorol. 152, 213–243.
Krpo, A., Salamanca, F., Martilli, A., Clappier, A., 2010. On the impact of anthropogenic heat fluxes on the urban boundary layer: a two-dimensional numerical study. Bound.-Layer Meteorol. 136, 105–127.
Kusaka, H., Kondo, H., Kikegawa, Y., Kimura, F., 2001. A Simple Single-Layer Urban Canopy Model For Atmospheric Models: Comparison With Multi-Layer And Slab Models. Bound.-Layer Meteorol. 101, 329–358.
Mills, G., 2009. Micro- and mesoclimatology. Prog. Phys. Geogr. 33, 711–717.
Lindberg, F., Grimmond, C.S.B., Yogeswaran, N., Kotthaus, S., Allen, L., 2013. Impact of city changes and weather on anthropogenic heat flux in Europe 1995–2015. Urban Clim. 4, 1–15, http://dx.doi.org/10.1016/j.uclim.2013.03.002.
Mlawer, E.J., Taubman, S.J., Brown, P.D., Iacono, M.J., Clough, S.A., 1997. Radiative transfer for inhomogeneous atmospheres: RRTM: a validated correlated-k model for the longwave. J. Geophys. Res. 102 (D14), 16663–16682.
Molenaar, R.E., Heusinkveld, B.G., Steeneveld, G.J., 2016. Projection of rural and urban human thermal comfort in The Netherlands for 2050. Int. J. Climatol. 36, 1708–1723.
Morabito, M., Crisci, A., Messeri, A., Capecchi, V., Modesti, PA, Gensini, GF, Orlandini, S., 2014. Environmental temperature and thermal indices: what is the most effective predictor of heat-related mortality in different geographical contexts? Sci. World J. 2014, 15, http://dx.doi.org/10.1155/2014/961750, Article ID 961750.
Oke, T.R., 1982. The energetic basis of the urban heat island. Q. J. R. Meteorol. Soc. 108, 1–24.
Powell, H., Lee, D., Bowman, A., 2012. Estimating constrained concentration-response functions between air pollution and health. Environmetrics 23, 228–237.
Rainham, D.G., Smoyer-Tomic, K.E., 2003. The role of air pollution in the relationship between a heat stress index and human mortality in Toronto. Environ. Res. 93, 9–19.
Skamarock, W.C., Klemp, J.B., Dudhia, J., Gill, D.O., Barker, D.M., Duda, M.G., Huang, X.-Y., Wang, W., Powers, J.G., 2008. A Description of the Advanced Research WRF Version 3, NCAR Technical Note NCAR/TN-475+STR. Boulder, USA.
Smargiassi, A., Goldberg, M.S., Plante, C., Fournier, M., Baudouin, Y., Kosatsky, T., 2009. Variation of daily warm season mortality as a function of micro-urban heat islands. J. Epidemiol. Community Health 63, 659–664.
Smoyer, K.E., 1998. Putting risk in its place: methodological considerations for investigating extreme event health risk. Soc. Sci. Med. 47, 1809–1824.
Souch, C., Grimmond, S., 2006. Applied climatology: urban climate. Prog. Phys. Geogr. 30, 270–279.
Steele, C.J., Dorling, S.R., von Glasow, R., Bacon, J., 2015. Modelling sea-breeze climatologies and interactions on coasts in the southern North Sea: implications for offshore wind energy. Q.J.R. Meteorol. Soc. 141, 1821–1835.
Steeneveld, G.J., Koopmans, S., Heusinkveld, B.G., van Hove, L.W.A., Holtslag, A.A.M., 2011a. Quantifying urban heat island effects and human comfort for cities of variable size and urban morphology in the Netherlands. J. Geophys. Res. 116 (2011JD015988).
Steeneveld, G.J., Tolk, L.F., Moene, A.F., Hartogensis, O.K., Peters, W., Holtslag, A.A.M., 2011b. Confronting the WRF and RAMS mesoscale models with innovative observations in the Netherlands-evaluating the boundary-layer heat budget. J. Geophys. Res. 116, D23114, http://dx.doi.org/10.1029/2011JD016303.
Sterk, H.A.M., Steeneveld, G.J., Vihma, T., Anderson, P.S., Bosveld, F.C., Holtslag, A.A.M., 2015. Clear-sky stable boundary layers with low winds over snow-covered surfaces. Part 1: WRF model evaluation. Q. J. R. Meteorol. Soc. 141, 2165–2184.
Stewart, I.D., Oke, T.R., 2012. Local climate zones for urban temperature studies. Bull. Am. Meteorol. Soc. 93, 1879–1900.
Synnefa, A., Dandou, A., Santamouris, M., Tombrou, M., Soulakellis, N., 2008. On the use of cool materials as a heat island mitigation strategy. J. Appl. Meteorol. Climatol. 47, 2846–2856.
Tan, J., Zheng, Y., Tang, X., Guo, C., Li, L., Song, G., Zhen, X., Yuan, D., Kalkstein, A.J., Li, F., 2010. The urban heat island and its impact on heat waves and human health in Shanghai. Int. J. Biometeorol. 54, 75–84.
Theeuwes, N.E., Steeneveld, G.J., Ronda, R.J., Heusinkveld, B.G., van Hove, L.W.A., Holtslag, A.A.M., 2014. Seasonal influence of street canyon aspect ratios on the urban heat island. Q. J. R. Meteorol. Soc. 140, 2197–2210.
Theeuwes, N.E., Steeneveld, G.J., Ronda, R.J., Rotach, M.W., Holtslag, A.A.M., 2015. Cool city mornings by urban heat. Environ. Res. Lett. 10, 114022.
Touloumi, G., Atkinson, R., Tertre, A.L., Samoli, E., Schwartz, J., Schindler, C., Vonk, J.M., Rossi, G., Saez, M., Rabszenko, D., Katsouyanni, K., 2004. Analysis of health outcome time series data in epidemiological studies. Environmetrics 15, 101–117.
Urban, A., Kyselý, J., 2014. Comparison of UTCI with other thermal indices in the assessment of heat and cold effects on cardiovascular mortality in the Czech Republic. Int. J Environ. Res. Public Health 11, 952–967.
Vandentorren, S., Suzan, F., Medina, S., Pascal, M., Maulpoix, A., Cohen, J.C., Ledrans, M., 2004. Mortality in 13 French cities during the August 2003 heat wave. Am. J. Public Health 94, 1518–1520.
Vandentorren, S., Bretin, P., Zeghnoun, A., Mandereau-Bruno, L., Croisier, A., Cochet, C., Ledrans, M., 2006. August 2003 heat wave in France: risk factors for death of elderly people living at home. Eur. J. Public Health 16, 583–591.
Vanos, J.K., 2015. Children's health and vulnerability in outdoor microclimates: a comprehensive review. Environ. Int. 76, 1–15.

WHO, 2006. Air Quality Guidelines: Global Update 2005 2006, Available online: http://www.euro.who.int/...data/assets/pdf_file/0005/78638/E90038.pdf.
WHO-Europe, 2008. Health Risks of Ozone from Long-range Transboundary Air Pollution, ISBN 978 92 890 42895.
Watkins, R., Palmer, J., Kolokotromi, M., 2007. Increased temperature and intensification of the urban heat island: implications for human comfort and urban design. Built Environ. 33, 85–96.
Wei, Y., Zhang, J., Li, Z., Gow, A., Chung, K.F., Hu, M., Sun, Z., Zeng, L., Zhu, T., Jia, G., Li, X., Duarte, M., Tang, X., 2016. Chronic exposure to air pollution particles increases the risk of obesity and metabolic syndrome: findings from a natural experiment in Beijing. FASEB J. 30, In press.
Zander, K.K., Botzen, W.J.W., Oppermann, E., Kjellstrom, T., Garnett, S.T., 2015. Heat stress causes substantial labour productivity loss in Australia. Nat. Clim. Change 5, 647–651.